Clustering of Massive Ensemble of Vehicle Trajectories in Strong, Dynamic and Uncertain Ocean Flows

Arkopal Dutt*, Deepak N. Subramani*, Chinmay S. Kulkarni*, Pierre F. J. Lermusiaux*†

*Department of Mechanical Engineering, Massachusetts Institute of Technology,
77 Massachusetts Avenue, Cambridge, MA 02139
†Corresponding author: pierrel@mit.edu

***Abstract*—Recent advances in probabilistic forecasting of regional ocean dynamics, and stochastic optimal path planning with massive ensembles motivate principled analysis of their large datasets. Specifically, stochastic time-optimal path planning in strong, dynamic and uncertain ocean flows produces a massive dataset of the stochastic distribution of exact time-optimal trajectories. To synthesize such big data and draw insights, we apply machine learning and data mining algorithms. Particularly, clustering of the time-optimal trajectories is important to describe their PDFs, identify representative paths, and compute and optimize risk of following these paths. In the present paper, we explore the use of hierarchical clustering algorithms along with a dissimilarity matrix computed from the pairwise discrete Frechet distance between all the optimal trajectories. We apply the algorithms to two datasets of massive ensembles of vehicle trajectories in a stochastic flow past a circular island and stochastic wind driven double gyre flow. These paths are computed by solving our dynamically orthogonal level set equations. Hierarchical clustering is applied to the two datasets, and results are qualitatively and quantitatively analyzed.**

I. Introduction

Autonomous ocean platforms are increasingly being used for several applications including ocean science research, resource discovery, ecosystem monitoring, and coastal security. For their efficient and economic operations, optimal planning of autonomous missions while rigorously accounting for uncertain, strong and dynamic ocean currents is necessary. Typically, passive ocean measuring platforms (e.g., drifters and buoys) move only due to advection by the currents. Even for the active ocean vehicles (e.g., gliders and Autonomous Underwater Vehicles) advection by currents is significant as these vehicles operate at a nominal speed that is of the order of the ocean currents. In fact, predicting and utilizing the currents to plan optimal paths leads to significant reduction in time and energy requirements for autonomous missions. Recently, we developed fundamental stochastic partial differential equations that govern the stochastic reachability and time-optimal paths in strong, dynamic and uncertain ocean currents [1], building off our earlier work in PDE-based time [2], and energy [3] optimal planning in realistic re-analysis and in real-time with real AUVs [4]. We point the readers to refs. [5, 6] for detailed reviews. Drifters and floats are ideal for economical data collection with large spatio-temporal coverage, e.g., the Argo float program [7]. Predicting the probabilistic reachability of these passive platforms is important for recovery and safe operation of assets (e.g., [8]). With the development of probabilistic regional ocean forecasting using dynamically orthogonal primitive equations [9], simulating an extremely large number of realizations of the ocean currents is currently feasible, and these can be utilized to simulate a large number of drifter and float trajectories. To synthesize such big data and produce meaningful analysis, we must do pattern recognition and clustering on the data sets of time-optimal vehicle trajectories and passive drifter trajectories. Clustering may also be applied in such cases for visualization, understanding the most probable ocean states, and to form PDF of trajectories for use in Lagrangian data assimilation [10]. Moreover, as ‘ocean of things’ expands and data sets grow, clustering and other learning techniques will become ubiquitous in ocean science and engineering.

The traditional application of trajectory clustering has been to video surveillance data, traffic footage [11, 12], and behavior monitoring [13] but it has recently become more popular in atmospheric and ocean sciences. It has been used to understand trends of tropical cyclones in the Northern Pacific [14], to understand climatology of long-range atmospheric transport [15], to identify patterns of eddies [16], for maritime traffic monitoring [17, 18], and to identify patterns in transmission loss in stochastic acoustic forecasts [19]. For an overall review, we refer the readers to [20, 21]. The main distinction between vehicle trajectories on land and in the ocean is the influence of ocean currents and dynamics. In order to obtain patterns of stochastic optimal trajectories, it is important to combine rigorous PDE based predictions of trajectories with clustering analysis.

The goal of the present paper is to develop a principled approach to perform hierarchical clustering of ensembles of time-optimal vehicle trajectories in uncertain ocean flows and study their properties. Through hierarchical clustering, we can gain insight into the underlying structure of the data at each level which cannot be obtained through density clustering. We employ a hierarchical clustering approach with a dissimilarity matrix computed from the pair-wise discrete Frechet distance [22, 23] between trajectories. Further, we show how representative paths for each cluster can be defined and illustrate their applications.

The layout of the paper is follows: In Section II-A, we briefly describe how the ensemble of time-optimal paths were computed by solving the stochastic time-optimal dynamically orthogonal equations. In Section II-B, the general methodology of agglomerative hierarchical clustering is described and how we apply it to our datasets. The application of this to two stochastic time-optimal trajectory datasets is described in III with results and future extensions of this work presented in IV.

II. Approach

A. Generation of Ensemble of Stochastic Time-Optimal Paths

We employ our stochastic dynamically orthogonal level set equations with uncertain velocity to predict the distribution of stochastic time-optimal paths. Here, we will briefly describe the approach and refer the readers to ref. [1] for details on the theory, numerical schemes and implementation.

For a vehicle navigating with a nominal relative speed $F(t)$ between two points $\mathbf{x}_s$ and $\mathbf{x}_f$ in a strong, dynamic, and uncertain flow $\mathbf{v}(\mathbf{x}, t; \omega)$, where ω is a random event, the stochastic reachability front tracking level-set field $\phi(\mathbf{x}, t; \omega)$ is governed by the stochastic Hamilton-Jacobi partial differential equation

$$\frac{\partial \phi(\mathbf{x}, t; \omega)}{\partial t} + F(t)|\nabla \phi(\mathbf{x}, t; \omega)| + \mathbf{v}(\mathbf{x}, t; \omega) \cdot \nabla \phi(\mathbf{x}, t; \omega) = 0\,, \tag{1}$$

with the initial condition as $\phi(\mathbf{x}, 0; \omega) = |\mathbf{x} - \mathbf{x}_s|$ and open boundary conditions as needed. The zero contour of the level set field tracks the reachability front of a vehicle start at $\mathbf{x}_s$ at time $t = 0$, and the first time this reachability front reaches the target $\mathbf{x}_f$ is the optimal arrival time $T(\mathbf{x}_f; \omega)$. From the time-series of zero contours of the level set field, the time-optimal track $\mathbf{X}_P(\mathbf{x}_s, t; \omega)$ can be computed by solving the vehicle backtracking path PDE,

$$\begin{aligned} \frac{d\mathbf{X}_P}{dt} &= -\mathbf{v}(\mathbf{X}_P, t; \omega) - F(t)\frac{\nabla \phi(\mathbf{X}_P, t; \omega)}{|\nabla \phi(\mathbf{X}_P, t; \omega)|}, \\ & 0 \le t \le T(\mathbf{x}_f; \omega) \text{ and } \mathbf{X}_P(\mathbf{x}_s, T; \omega) = \mathbf{x}_f\,. \end{aligned} \tag{2}$$

Solving the stochastic PDE (1) is expensive by traditional Monte Carlo methods, and hence, we utilize their variance-optimal reduced order dynamically orthogonal equations, which shadow the dominant uncertainties to predict the stochastic distribution with massive ensemble sizes. We need to integrate only a few mode PDEs (which are the same cost as one evaluation of the forward model in a Monte Carlo simulation) and a large number of coefficient ODEs (which are inexpensive to integrate compared to the mode PDEs). The stochastic dynamically orthogonal level set equations and the numerical schemes to solve them, including verification and validation, are provided in ref. [1].

For the applications in the present paper, we utilize the distribution of stochastic time-optimal paths predicted and described in ref. [1], but now for clustering analysis.

B. Clustering

Once an ensemble of trajectories is obtained, different dissimilarity matrices can be generated considering various distance metrics defined between any two trajectories. An agglomerative hierarchical clustering algorithm is then used to partition the ensemble of trajectories into a certain number of clusters, based on the dissimilarity matrix. A number of questions arise such as which distance metric to prefer in constructing a dissimilarity matrix, which linkage method is suitable for the problem we are interested in and the number of clusters required to adequately represent our data.

Popular distance metrics include the Euclidean distance, Hausdorff distance [24], Bhattacharyya distance [25], Frechet distance [22, 23], Dynamic Time Warping distance [26], and Longest Common Subsequence distance [27–29]. When assessing the distances between two trajectories from an ensemble of time-optimal trajectories, it is important to account for both spatial and temporal information. Two vehicle trajectories may be similar when looking at spatial information but may not be similar when considering their temporal information because of the different dynamics they encountered and the temporal domain in which they were simulated. For our case, we use the discrete Frechet distance as our metric as it takes into account both location and time ordering unlike Euclidean or Hausdorff distance. It is also possible to consider multiple dissimilarity matrices generated from different distance metrics and adopt an ensembling approach [30] during clustering which we do not discuss here.

There exists variety of heuristics to prefer the single, complete, weighted or unweighted average linkage methods. Some insight into which method to prefer comes from recent progress in development of a cost function for dissimilarity based hierarchical clustering algorithms [31]. Further, [31] showed that a simple recursive sparsest-cut based approach achieves an $\mathcal{O}(\log^{3/2} n)$ approximation on worst-case inputs. A refined analysis in [32] showed that it actually achieves an $\mathcal{O}(\sqrt{\log n})$ approximation. Moreover, [32] showed that the average linkage method gives a factor 2 approximation, making it a practical algorithm. Another reason to prefer the average linkage method is its comparable robust performance in presence of outliers [33]. As the average linkage method doesn't suffer from chaining or crowding, usually compact and distinct clusters are obtained.

Determining the number of clusters to use to represent the underlying structure of the data is a challenging problem. One ideally wishes to minimize the within-cluster variation and maximize the between-cluster variation. The gap statistic [34], silhouette distance [35], Aitken Information Criterion (AIC), and Bayesian Information Criterion (BIC) [36] are some of the commonly used methods for estimating the cluster size. A lot of these methods require that we keep the ensemble data in the workspace but in our case, the data is discarded and all the knowledge of the data is considered to be contained in the dissimilarity matrix. We thus use the silhouette distance to assess the quality of a clustering assignment. For the i^{th} data point, the silhouette is given by

$$s(i) = \frac{b(i) - a(i)}{\max(a(i), b(i))} \tag{3}$$

where $a(i)$ is the average dissimilarity between i^{th} data point and all the other points in the cluster that the i^{th} data point belongs to. If we denote $d(i, C)$ as the average dissimilarity between the i^{th} data point and all the other points in cluster C different from the cluster that the i^{th} data point belongs to, then $b(i) = \min_{C \in C_k} d(i, C)$. Clearly, the dissimilarity matrix and the clustering assignment is all that is required to calculate $s(i)$. Once $s(i)$ is known, the average silhouette distance can be used as a criteria to judge the quality of an assignment. A higher value indicates a better clustering assignment.

III. Application of Clustering

A. Datasets of Stochastic Time-Optimal Trajectories

We primarily use two datasets of massive ensembles of stochastic time-optimal trajectories shown in Fig. 1, computed using our stochastic time-optimal path planning S-PDEs (sec. II-A and reported in ref. [1]). The first dataset (Fig. 1a) is the ensemble of stochastic time-optimal trajectories in a flow past a circular island (Test Case 3 of ref. [1]), and the second dataset (Fig. 1b) is the ensemble of stochastic time-optimal trajectories in a stochastic wind-driven double gyre flow (Test Case 2 of ref. [1]). In the first, the stochastic flow field is obtained by solving the stochastic quasi geostrophic flow past a circular island of diameter 1 km in a channel of size 16 km x 6 km with uncertain initial conditions. Utilizing this uncertain velocity forecast, the stochastic dynamically orthogonal equations are solved, and the dataset of the distribution of stochastic time-optimal paths with 10,000 realizations is obtained. The AUV travels from a point directly upstream from the island to a point directly downstream (Target 5 of Test Case 3 in ref. [1]). In the second, the stochastic quasi geostrophic equations are solved in a basin of 1000 km x 1000 km and forced by a wind from west to east, with uncertain initial conditions. As before, the dataset of stochastic time-optimal trajectories, now with 5,000 realizations is obtained. In this figure, the circular marker represents the start location of the AUV and the star marker represents the target.

Next, we apply the hierarchical clustering algorithm (Sec. II-B) on these two datasets one-by-one.

B. Hierarchical Clustering on Dataset 1

We first compute the dissimilarity matrix over the time-optimal vehicle trajectories (shown in Fig. 1a) using the metric of discrete Frechet distance. A dendogram tree (shown in Fig. 2) is created using the dissimilarity matrix through the agglomerative hierarchical clustering algorithm with average linkage. In the Fig. 2, we have colored two distinct clusters and shown the dendogram with a granularity of 50 clusters to aid visualization. On an average, the trajectories belonging to the same cluster are more similar to each other than those belonging to another cluster. According to the number of clusters we wish to identify, the tree can be cut at different heights.

Once a clustering assignment has been made, we want to identify the representative trajectories of each cluster. The representative trajectory in each cluster is considered to be the realization nearest to all the other trajectories within the cluster, corresponding to the realization with the minimum row sum in the dissimilarity matrix. This definition of a rep-

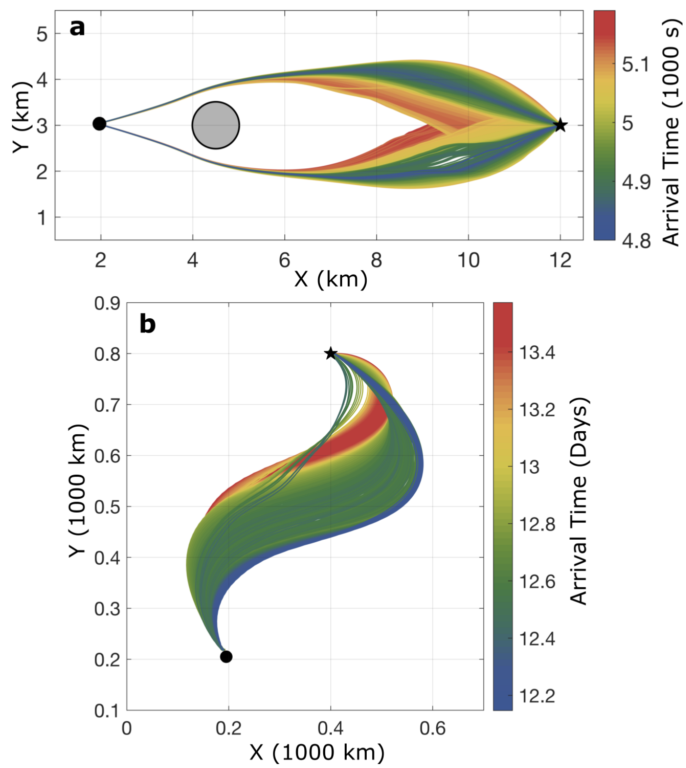

Fig. 1. (**a**) *Dataset 1*: Distribution of stochastic time-optimal paths for the stochastic flow past a circular island in a channel. (**b**) *Dataset 2*: Distribution of stochastic time-optimal paths for the stochastic wind driven double gyre flow. Figure panels adapted from [1].

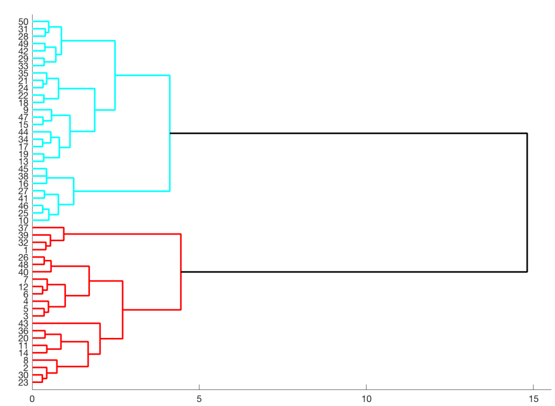

Fig. 2. *Dataset 1*: Dendrogram obtained through hierarchical clustering algorithm applied on the dissimilarity matrix (2 clusters colored).

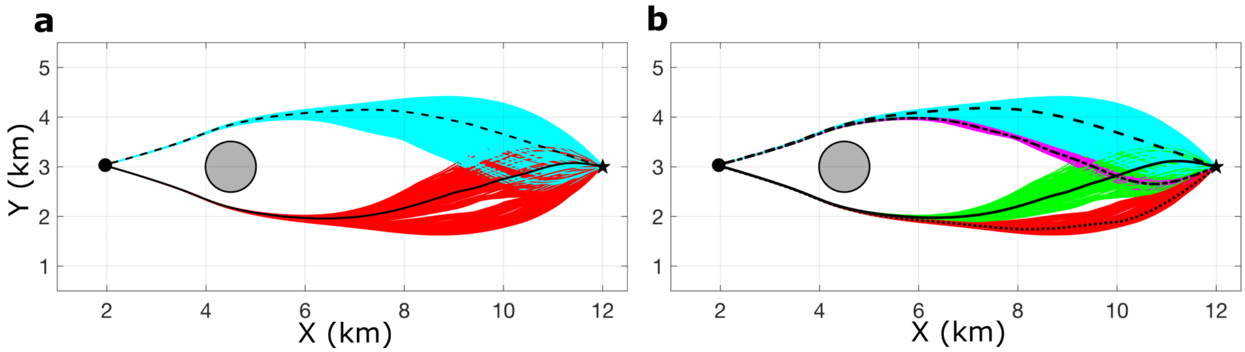

Fig. 3. *Dataset 1*: (**a**) Clusters of vehicle paths shown by color with representative paths of each cluster colored in black ('-' is for cluster 1, '–' is for cluster 2). (**b**) Clusters of vehicle paths shown by color with representative paths of each cluster colored in black ('-' is for cluster 1, '–' is for cluster 2, ':' is for cluster 3, '-.' is for cluster 4).

resentative trajectory ensures that this is a realizable predicted trajectory.

Fig. 3a and Fig. 3b shows the clustering obtained with two and four clusters respectively. In the former, the clusters correspond to the northern and southern trajectories. In the latter, further sub-clusters are identified – two to the north of the island and two to the south. We observe that the spatial information plays a more important role in the clustering assignments for each trajectory than temporal information. Paths with different arrival times but similar spatial lengths and shapes belong to the same cluster. Moreover, we observe that the representative paths of each cluster are not necessarily the mean paths of the clusters.

From visual inspection, it appears that two clusters adequately represent the data. We confirm this by plotting the trend of average silhouette distance with the number of clusters in Fig. 4. We observe that it is maximized for a cluster size of two. The probability of a trajectory belonging to a particular cluster is proportional to the number of trajectories assigned to that cluster. This may in turn aid in computing risk each trajectory and identifying risk-optimal paths [9].

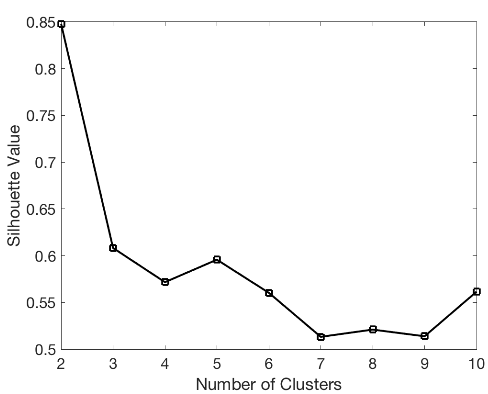

Fig. 4. *Dataset 1*: Trend of average silhouette distance with number of clusters

It may be beneficial to represent the data with more clusters when the purpose is to extract the spatial PDF of the time-optimal trajectories. By utilizing 40 clusters, a PMF map can be generated as shown in Fig. 5. In this figure, each cluster's representative path is colored by its probability of occurrence as the fraction of the number of realizations in that cluster. Such a probability description of the paths is very helpful for visualization as well as for quick computation of spatial statistics with only the representative paths and their probabilities. In this case, now the PDF of the paths that were earlier captured with 10,000 realizations each with a probability of 1/10,000 is now replaced with 40 representative paths each with its own probabilities. In other words, we have used clustering to do a relevant sub-sampling of the massive ensemble of time-optimal trajectories.

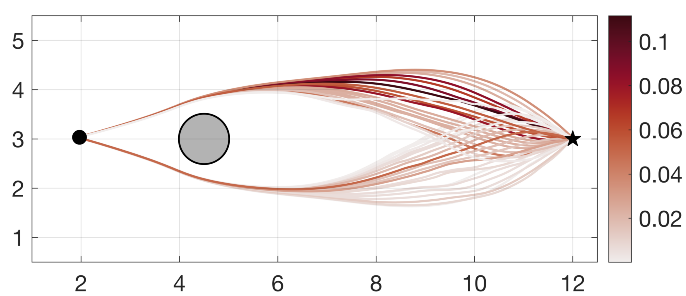

Fig. 5. *Dataset 1*: Representative paths colored by the probability of the clusters they represent.

C. Hierarchical Clustering on Dataset 2

As for dataset 1, we first compute the dissimilarity matrix over the time-optimal vehicle trajectories of the dataset 2 (shown in Fig. 1b) using the metric of discrete Frechet distance. A dendogram tree (shown in Fig. 6) is created using the dissimilarity matrix through the agglomerative hierarchical clustering algorithm with average linkage. As before, to aid visualization for the purpose of illustration, we have colored four distinct clusters and shown only up to 50 clusters in Fig. 6. Note that, from the 50 clusters at which we stopped, further branches and nodes exist going all the way up to the 5000 realizations in our dataset.

Fig. 7 shows three panels with two, three and four clusters, and their representative paths. Fig. 7a has two clusters, with

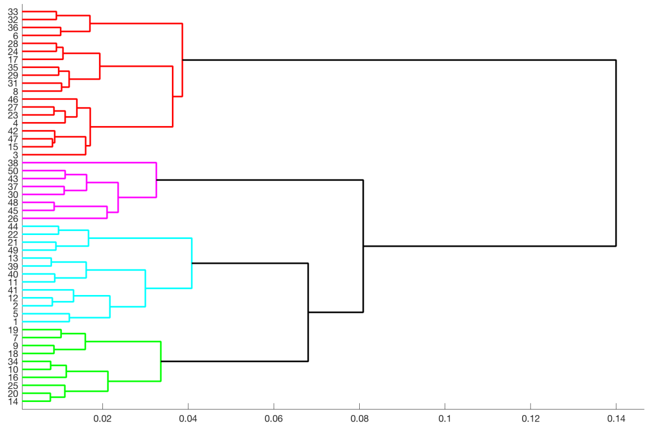

Fig. 6. *Dataset 2*: Dendrogram obtained through hierarchical clustering algorithm applied on the dissimilarity matrix.

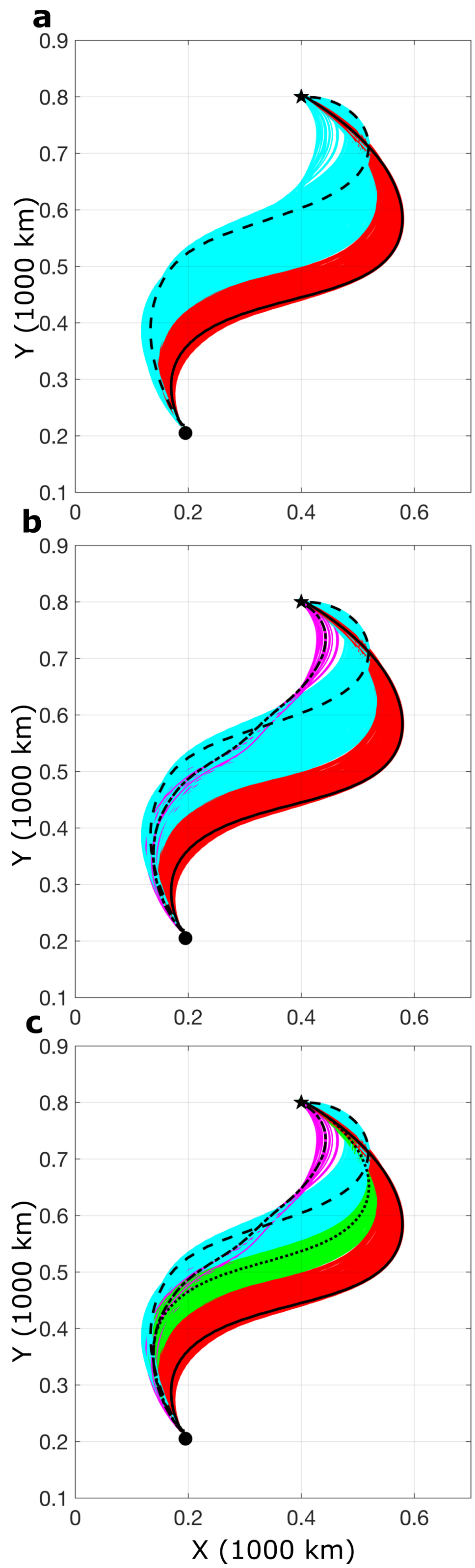

Fig. 7. *Dataset 2*: (**a**) Clusters of vehicle paths shown by color with representative paths of each cluster colored in black ('-' is for cluster 1, '–' is for cluster 2). (**b**) Clusters of vehicle paths shown by color with representative paths of each cluster colored in black ('-' is for cluster 1, '–' is for cluster 2, ':' is for cluster 3). (**c**) Clusters of vehicle paths shown by color with representative paths of each cluster colored in black ('-' is for cluster 1, '–' is for cluster 2, ':' is for cluster 3, '-.' is for cluster 4).

paths belonging to each colored in cyan and red. When three clusters are utilized, the cyan cluster is further divided into two clusters as shown in Fig. 3b, and when four clusters are utilized, the cyan cluster is further divided into three as shown in Fig. 7c. This fact is also observable in the dendogram (Fig. 2) where we can see that the red colored cluster is not changing, whereas the branch corresponding to the other cluster gets subdivided when more clusters are utilized.

Fig. 8 shows the representative paths colored by the probabilities of their clusters. The probability of the representative path is highest for the path marked 1, followed by path marked 2. We note that these two paths are in fact the representative paths of the first two clusters shown in Fig. 7a.

IV. Conclusion and Future Work

This work presents how hierarchical clustering can be used on ensembles of optimal paths obtained from stochastic ocean model predictions. Firstly, we discussed how the ensemble of stochastic time-optimal paths were generated. This was followed by a discussion of the considerations we made when applying a hierarchical clustering algorithm to two datasets of massive ensemble of time-optimal trajectories computed by solving our stochastic dynamically orthogonal level set equations in strong, dynamic, and uncertain flow fields. Results from the clustering are analyzed from the perspective of dynamics of the flow and the properties of the time-optimal paths. The clustering analysis enables us to draw insights about the dataset, and also aid in quick computations of spatial statistics. In the future, this clustering analysis can be utilized for several more applications. For example, once a set of clusters is defined on a typical dataset, new incoming model vehicle trajectories can be classified into one of these clusters through nearest neighboring algorithms. Such an approach will also help in detecting anomalous trajectories that may correspond to rare events of the stochastic model simulation.

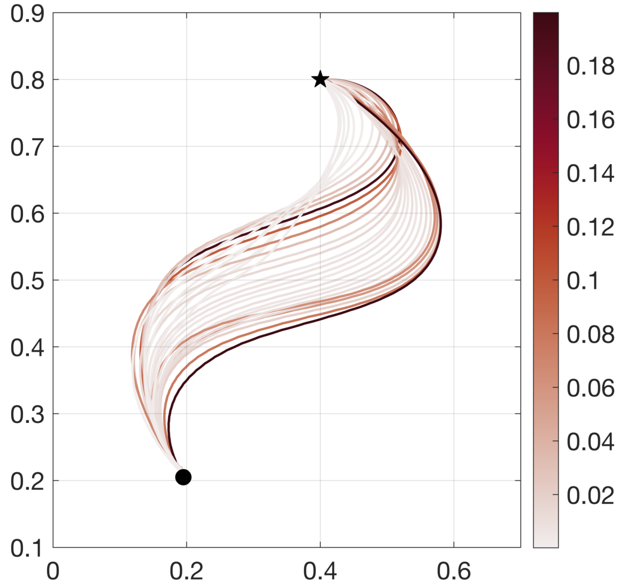

Fig. 8. *Dataset 2*: Representative paths colored by the probability of the clusters they represent.

Other avenues of future work include applying clustering for designing probabilistic policies for optimal operations (e.g., risk-optimal planning), examining relationships between clusters of time-optimal paths and that of the underlying flow field. Overall, the application of machine learning approaches with rigorous fundamental planning PDEs and uncertainty quantification opens up new exciting avenues of research and development in ocean science and engineering.

Acknowledgment

We thank our MIT MSEAS group for the insightful discussions. We are grateful to the Office of Naval Research for support under Grants N00014-14-1-0476 (Science of Autonomy - LEARNS) to Massachusetts Institute of Technology (MIT). We also thank the MIT Tata Center for the fellowship support to DNS.

References

[1] D. N. Subramani, Q. J. Wei, and P. F. J. Lermusiaux, "Stochastic time-optimal path-planning in uncertain, strong, and dynamic flows," *Computer Methods in Applied Mechanics and Engineering*, vol. 333, pp. 218–237, 2018.

[2] T. Lolla, P. J. Haley, Jr., and P. F. J. Lermusiaux, "Time-optimal path planning in dynamic flows using level set equations: Realistic applications," *Ocean Dynamics*, vol. 64, no. 10, pp. 1399–1417, 2014.

[3] D. N. Subramani, P. J. Haley, Jr., and P. F. J. Lermusiaux, "Energy-optimal path planning in the coastal ocean," *Journal of Geophysical Research: Oceans*, vol. 122, pp. 3981–4003, 2017.

[4] D. N. Subramani, P. F. J. Lermusiaux, P. J. Haley, Jr., C. Mirabito, S. Jana, C. S. Kulkarni, A. Girard, D. Wickman, J. Edwards, and J. Smith, "Time-optimal path planning: Real-time sea exercises," in *Oceans '17 MTS/IEEE Conference*, Aberdeen, Jun. 2017.

[5] P. F. J. Lermusiaux, D. N. Subramani, J. Lin, C. S. Kulkarni, A. Gupta, A. Dutt, T. Lolla, P. J. Haley, Jr., W. H. Ali, C. Mirabito, and S. Jana, "A future for intelligent autonomous ocean observing systems," *Journal of Marine Research*, vol. 75, no. 6, pp. 765–813, Nov. 2017, the Sea. Volume 17, The Science of Ocean Prediction, Part 2.

[6] P. F. J. Lermusiaux, T. Lolla, P. J. Haley, Jr., K. Yigit, M. P. Ueckermann, T. Sondergaard, and W. G. Leslie, "Science of autonomy: Time-optimal path planning and adaptive sampling for swarms of ocean vehicles," in *Springer Handbook of Ocean Engineering: Autonomous Ocean Vehicles, Subsystems and Control*, T. Curtin, Ed. Springer, 2016, ch. 21, pp. 481–498.

[7] D. Roemmich, G. C. Johnson, S. Riser, R. Davis, J. Gilson, W. B. Owens, S. L. Garzoli, C. Schmid, and M. Ignaszewski, "The argo program: Observing the global ocean with profiling floats," *Oceanography*, vol. 22, no. 2, pp. 34–43, 2009.

[8] P. F. J. Lermusiaux, P. J. Haley, Jr., S. Jana, A. Gupta, C. S. Kulkarni, C. Mirabito, W. H. Ali, D. N. Subramani, A. Dutt, J. Lin, A. Shcherbina, C. Lee, and A. Gangopadhyay, "Optimal planning and sampling predictions for autonomous and lagrangian platforms and sensors in the northern Arabian Sea," *Oceanography*, vol. 30, no. 2, pp. 172–185, Jun. 2017, special issue on Autonomous and Lagrangian Platforms and Sensors (ALPS).

[9] D. N. Subramani, "Probabilistic regional ocean predictions: Stochastic fields and optimal planning," Ph.D. dissertation, Massachusetts Institute of Technology, Department of Mechanical Engineering, Cambridge, Massachusetts, Feb. 2018.

[10] A. Dutt, "High order stochastic transport and Lagrangian data assimilation," Master's thesis, Massachusetts Institute of Technology, Department of Mechanical Engineering, Cambridge, Massachusetts, Feb. 2018.

[11] S. Atev, G. Miller, and N. P. Papanikolopoulos, "Clustering of vehicle trajectories," *IEEE Transactions on Intelligent Transportation Systems*, vol. 11, no. 3, pp. 647–657, 2010.

[12] Z. Fu, W. Hu, and T. Tan, "Similarity based vehicle trajectory clustering and anomaly detection," in *Image Processing, 2005. ICIP 2005. IEEE International Conference on*, vol. 2. IEEE, 2005, pp. II–602.

[13] M. Gariel, A. N. Srivastava, and E. Feron, "Trajectory clustering and an application to airspace monitoring," *IEEE Transactions on Intelligent Transportation Systems*, vol. 12, no. 4, pp. 1511–1524, 2011.

[14] S. J. Camargo, A. W. Robertson, S. J. Gaffney, P. Smyth, and M. Ghil, "Cluster analysis of typhoon tracks. part i: General properties," *Journal of Climate*, vol. 20, no. 14, pp. 3635–3653, 2007.

[15] J. M. Harris and J. D. Kahl, "A descriptive atmospheric transport climatology for the mauna loa observatory,

using clustered trajectories," *Journal of Geophysical Research: Atmospheres*, vol. 95, no. D9, pp. 13 651–13 667, 1990.

[16] Y. Mo, D. Wu, and Y. Du, "Application of trajectory clustering and regionalization to ocean eddies in the south china sea," in *Spatial Data Mining and Geographical Knowledge Services (ICSDM), 2015 2nd IEEE International Conference on*. IEEE, 2015, pp. 45–48.

[17] B. Liu, E. N. de Souza, S. Matwin, and M. Sydow, "Knowledge-based clustering of ship trajectories using density-based approach," in *Big Data (Big Data), 2014 IEEE International Conference on*. IEEE, 2014, pp. 603–608.

[18] A. Dahlbom and L. Niklasson, "Trajectory clustering for coastal surveillance," in *Information Fusion, 2007 10th International Conference on*. IEEE, 2007, pp. 1–8.

[19] M. M. Swezey, "Ocean acoustic uncertainty for submarine applications," Master's thesis, Massachusetts Institute of Technology, Department of Mechanical Engineering, Cambridge, Massachusetts, Jun. 2016.

[20] Y. Zheng, "Trajectory data mining: an overview," *ACM Transactions on Intelligent Systems and Technology (TIST)*, vol. 6, no. 3, p. 29, 2015.

[21] J. Bian, D. Tian, Y. Tang, and D. Tao, "A survey on trajectory clustering analysis," *arXiv preprint arXiv:1802.06971*, 2018.

[22] F. Shao, S. Cai, and J. Gu, "A modified hausdorff distance based algorithm for 2-dimensional spatial trajectory matching," in *Computer Science and Education (ICCSE), 2010 5th International Conference on*. IEEE, 2010, pp. 166–172.

[23] D. N. Subramani and P. F. J. Lermusiaux, "Energy-optimal path planning by stochastic dynamically orthogonal level-set optimization," *Ocean Modeling*, vol. 100, pp. 57–77, 2016.

[24] J. Chen, R. Wang, L. Liu, and J. Song, "Clustering of trajectories based on hausdorff distance," in *Electronics, Communications and Control (ICECC), 2011 International Conference on*. IEEE, 2011, pp. 1940–1944.

[25] X. Li, W. Hu, and W. Hu, "A coarse-to-fine strategy for vehicle motion trajectory clustering," in *Pattern Recognition, 2006. ICPR 2006. 18th International Conference on*, vol. 1. IEEE, 2006, pp. 591–594.

[26] Z. Shao and Y. Li, "On integral invariants for effective 3-d motion trajectory matching and recognition." *IEEE Trans. Cybernetics*, vol. 46, no. 2, pp. 511–523, 2016.

[27] L. Bergroth, H. Hakonen, and T. Raita, "A survey of longest common subsequence algorithms," in *String Processing and Information Retrieval, 2000. SPIRE 2000. Proceedings. Seventh International Symposium on*. IEEE, 2000, pp. 39–48.

[28] M. Vlachos, G. Kollios, and D. Gunopulos, "Discovering similar multidimensional trajectories," in *Data Engineering, 2002. Proceedings. 18th International Conference on*. IEEE, 2002, pp. 673–684.

[29] J. Kim and H. S. Mahmassani, "Spatial and temporal characterization of travel patterns in a traffic network using vehicle trajectories," *Transportation Research Procedia*, vol. 9, pp. 164–184, 2015.

[30] S. Amiri, B. S. Clarke, and J. L. Clarke, "Clustering categorical data via ensembling dissimilarity matrices," *Journal of Computational and Graphical Statistics*, vol. 27, no. 1, pp. 195–208, 2018.

[31] S. Dasgupta, "A cost function for similarity-based hierarchical clustering," in *Proceedings of the forty-eighth annual ACM symposium on Theory of Computing*. ACM, 2016, pp. 118–127.

[32] V. Cohen-Addad, V. Kanade, F. Mallmann-Trenn, and C. Mathieu, "Hierarchical clustering: Objective functions and algorithms," in *Proceedings of the Twenty-Ninth Annual ACM-SIAM Symposium on Discrete Algorithms*. SIAM, 2018, pp. 378–397.

[33] M. Gagolewski, M. Bartoszuk, and A. Cena, "Genie: A new, fast, and outlier-resistant hierarchical clustering algorithm," *Information Sciences*, vol. 363, pp. 8–23, 2016.

[34] T. Hastie, R. Tibshirani, and G. Walther, "Estimating the number of data clusters via the gap statistic," *J Roy Stat Soc B*, vol. 63, pp. 411–423, 2001.

[35] P. J. Rousseeuw, "Silhouettes: a graphical aid to the interpretation and validation of cluster analysis," *Journal of computational and applied mathematics*, vol. 20, pp. 53–65, 1987.

[36] S. S. Chen and P. S. Gopalakrishnan, "Clustering via the bayesian information criterion with applications in speech recognition," in *Acoustics, Speech and Signal Processing, 1998. Proceedings of the 1998 IEEE International Conference on*, vol. 2. IEEE, 1998, pp. 645–648.